

DRIFT EFFECTS IN HgCdTe DETECTORS

B. PAVAN KUMAR¹, M. W. AKRAM^{1,*}, BAHNIMAN GHOSH¹,
JOSEPH JOHN²

¹Department of Electrical Eng., Indian Institute of Technology Kanpur, Kanpur-208016, India

²Department of Electrical Eng., Indian Institute of Technology Mumbai, Powai-400076, India

*Corresponding Author: mwakram@iitk.ac.in

Abstract

The characteristics of temporal drift in spectral responsivity of HgCdTe photodetectors is investigated and found to have an origin different from what has been reported in literature. Traditionally, the literature attributes the cause of drift due to the deposition of thin film of ice water on the active area of the cold detector. The source of drift as proposed in this paper is more critical owing to the difficulties in acquisition of infrared temperature measurements. A model explaining the drift phenomenon in HgCdTe detectors is described by considering the deep trapping of charge carriers and generation of radiation induced deep trap centers which are meta-stable in nature. A theoretical model is fitted to the experimental data. A comparison of the model with the experimental data shows that the radiation induced deep trap centers and charge trapping effects are mainly responsible for the drift phenomenon observed in HgCdTe detectors.

Keywords: HgCdTe, Spectral responsivity, Meta-stable traps, Quantum efficiency, Detectivity, Carrier lifetime.

1. Introduction

HgCdTe detectors are widely used in high speed infrared radiation measurements since it has high response speed. By varying the composition of x in $\text{Hg}_{1-x}\text{Cd}_x\text{Te}$ its bandgap can be tuned over a wide range (0-1.5 eV) and therefore it is a noteworthy material for detector applications over the entire IR range [1-4]. HgCdTe is a direct bandgap semiconductor with large optical absorption coefficient. In order to reduce the number of thermally generated minority carriers and also to obtain higher responsivity, HgCdTe detectors have to be operated at cryogenic temperature (~80 K). Stability of the spectral responsivity of photodetectors with time is an important requirement for accurate infrared

radiation measurements. These HgCdTe photo detectors are widely used over 3-5 μm wavelengths due to their higher responsivity and also offering low noise equivalent power (NEP) [1]. The stochastic nature of generation and recombination of charge carriers limits the performance of HgCdTe photodetectors. The response per unit incident radiant power of HgCdTe detectors shows wavelength dependence. To have a very fast response and perfect signal-to-noise ratio, the HgCdTe detectors need cooling.

Drift of spectral responsivity with time is observed in HgCdTe detectors. The characteristics of the drift are investigated and found to have an origin different from that reported in literature [5-8]. The drifts as reported in literature are caused due to the deposition of ice on the active area of the cold detector. Ice has a strong absorption coefficient approximately 3.1 μm and so the incident radiant power on the detector reaching the active area is depleted due to absorption of radiation by ice in between them. The increasing thickness of ice in front of the active area of the detector results in decrease in spectral responsivity of cryogenically cooled detectors at 3.1 μm wavelength. Analogous behaviour in the responsivity of HgCdTe detectors has also been observed in the regime of 11 to 13 μm wavelength. One of the authors [6] attributed the drift in spectral responsivity due to interaction of the thin film of ice (a dielectric film) with the multilayer dielectric anti-reflection coatings deposited on the active areas of HgCdTe detectors. These drifts could be reduced by regularly evacuating the detector Dewar by baking it at temperatures of 50 $^{\circ}\text{C}$ for approximately 48h. This ensured ice-free operation for a few weeks.

The aim of this paper is to report the causes of drift in HgCdTe detectors which is different from that reported in literature. The Dewar in which the detector is housed had been completely evacuated before the drifts were observed. This ensures that drifts observed have nothing to do with ice-formation. All the photoconductive (PC) HgCdTe detectors whose drift characteristics are subject of this paper, consists of 1 mm \times 1 mm active areas and is thermo-electric cooled. The source of drift as proposed in this paper is more critical owing to the difficulties in acquisition of infrared temperature measurements. In this work it is demonstrated that the source of new drift is due to charge trapping effects and generation of radiation induced deep trap centers which are meta-stable in nature [9-11]. Experiments and simulations have been carried out to ascertain the cause of the drift and a theoretical model has been proposed which explains the characteristics of the drift phenomenon. It has been shown that due to the variation of radiation induced deep trap centers, effective carrier lifetime in the semiconductor changes and hence the drift effects are being observed.

2. Experiments

2.1. Experimental setup

Figure 1 shows the block diagram of the experimental setup. The detector was placed in a chamber in front of infrared source. The incandescent bulbs of different intensities (40 W, 100 W, 200 W, 300 W) are used as infrared source [1-4]. These are ordinary incandescent bulbs used at households (made by M/s Philips India). These bulbs have peak emission in the 500-700 nm region with comparatively lower powers above the visible range (>750 nm). Judson J15D series HgCdTe photoconductive (PC) detector with three stage thermo-electric cooling is being used. The three stage thermo-electric cooler maintains the

detector at -65°C. LM35, a temperature sensor IC is placed in front of the detector to monitor the temperature of the chamber.

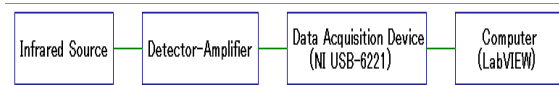


Fig. 1. Block Diagram of the Experimental Setup.

The model PA-300 current pre-amplifier is used in conjunction with J15D series HgCdTe detectors as shown in Fig 2. A National Instruments NI USB-6221, multifunction DAQ, is used to digitize the analog voltages. The output of the detector-amplifier and LM35 output are wired into appropriate channels of NI USB-6221 for data acquisition. The NI USB-6221 is connected to the computer which interacts with the controlling software programmed in LabVIEW. The program developed in LabVIEW is used to store data output of the detector over a period of time. Readings were taken for every 30 seconds over a period of approximately 6 hours. After the temperature gets stabilized inside the chamber due to incandescent bulb, the power to the detector is switched on and the output of the detector is recorded for a period of six hours. The experiments are conducted for different temperature measurements as shown in the Table 1 and are repeated to check reproducibility.

Table 1. Temperature of the Chamber Maintained due to Different Bulb Intensities.

S. No.	Bulb Intensities	Temperature of chamber
1	40 W	45°C
2	100 W	55°C
3	200 W	70°C
4	300 W	90°C

The first stage output voltage V_{out} of the detector is given by the following equation

$$V_{out} = (V_d - V_b) G_b R_f + (V_d R_f G_d) + V_d \tag{1}$$

It can be seen from Eq. (1) that V_{out} is a linear function of the photodetector conductance G_d . V_d is the voltage across the detector, R_f is the feedback resistor as shown in Fig. 2, R_b is the bias resistor, $G_b = (1/ R_b)$, and V_b is the voltage across bias resistor. $R_b = 2.64 \text{ K}\Omega$, $R_d = 230\Omega$, $R_{set} = 357 \Omega$.

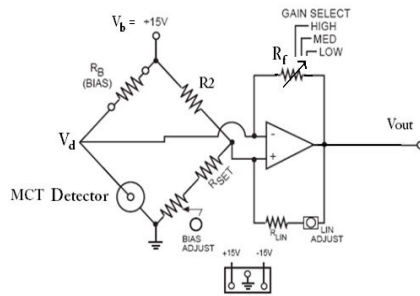


Fig. 2. PA-300 Preamp Equivalent Circuit.

2.2. Observations

The output voltage of the detector is observed to slowly drift with time as shown in Figs. 3 and 4, and the drift in output voltage for different temperatures is shown in Fig. 5. The resulting drifts are reproducible. It is observed that the amount of drift for different temperature measurements is dependent on the intensity of radiation. After running the device for a long time, it is switched off and put to on state again; output recovers to its initial values and starts to drift again. This suggests that the mechanism responsible for these drifts is reversible.

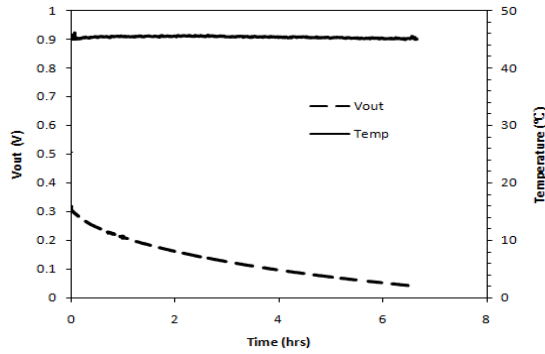


Fig. 3. Output Drift for a Temperature Measurement of 45°C.

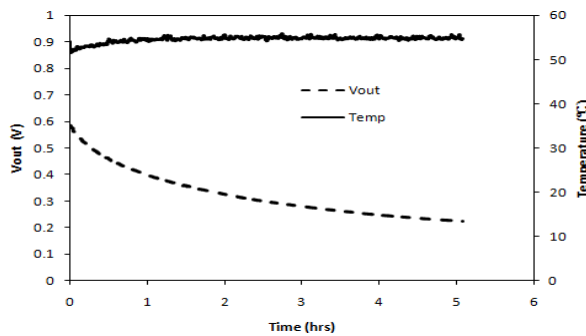


Fig. 4. Output Drift for a Temperature Measurement of 55°C.

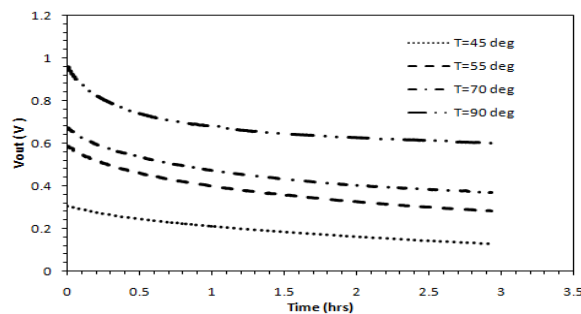


Fig. 5. Drift in Output Voltage for Various Temperature Measurements.

2.3. Discussions

This output voltage drift with time is attributed to the decrease in spectral responsivity of the detector with time. This decrease in responsivity is attributed not just due to trapping of charge carriers but also due to increased recombination through meta-stable trap centre's which are generated due to irradiation. The radiation induced defects take up a broad spectrum of energy levels within the semiconductor energy gap and act as recombination centers or electron trap centers that cause a change in free carrier concentration, mobility and carrier lifetime. Therefore, the increase in trap density results in increase in the resistance of the detector. The resistance variation with time is plotted for a temperature measurement of 70°C as observed from experiment shown in Fig. 6. The variation of resistance with trap density as estimated from simulations is shown in Fig. 7. The increased recombination due to radiation induced deep trap centers reduces the carrier-lifetime and hence reduces the gain and responsivity of the photoconductive detector. Since the output recovers to its initial values when the detector is switched on again, this suggests that radiation induced deep trap centers are meta-stable in nature.

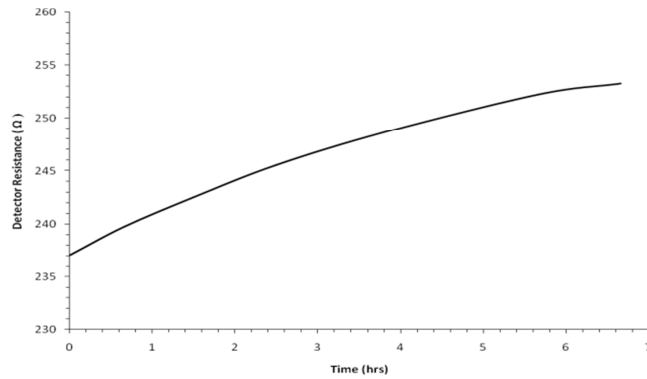


Fig. 6. Detector Resistance Variation due to Continuous-Wave Irradiation.

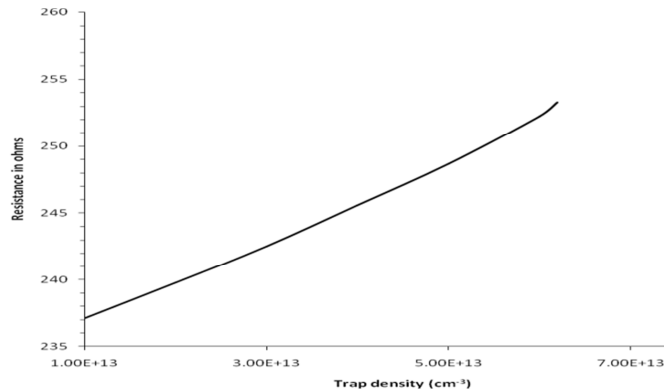


Fig. 7. Detector Resistance Variation with Trap Density.

3. Simulation

Numerical computations and simulations have been carried out using ATLAS Silvaco® for the theoretical characterization of an n-type Hg_{0.71}Cd_{0.29}Te photoconductive detector at an operating temperature of 208 K. Simulations are carried out to characterize drift phenomenon theoretically in the HgCdTe PC detectors. A program has been developed for simulation of a two dimensional photoconductive detector. The photoconductive detector consists of an n-type Hg_{0.71}Cd_{0.29}Te photoconductor grown on sapphire substrate. The parameters used in simulation are shown in Table 2. I-V characteristics have been plotted for increasing trap densities. The resistances calculated from the slopes of these I-V curves are matched to the experimental data (Resistance variation with time). The plot of resistance variation with trap density is shown in Fig. 7. The simulated data stored in .log files is extracted using Origin tool and then from the extracted data's, the quantum efficiency is plotted. The photoconductive gain, 'g', in a photoconductive detector defined as the ratio of the carrier lifetime to the transit time of charge carriers, also decreases due to decrease in carrier lifetime.

Table 2. Parameters Used in Simulation.

Parameter	Values
n-type Hg _{1-x} Cd _x Te	$X = 0.2915$
Operating Temperature	208 K
Bandgap Energy (E_g)	0.2583 eV
Cut-off wavelength (λ_c)	4.8 μm
Length (l)	50 μm
Width (w)	50 μm
Thickness (t)	10 μm
Intrinsic carrier concentration	$3.387 \times 10^{14} \text{ cm}^{-3}$
Capture cross section (σ_p, σ_n)	10^{-16} cm^2
Background photon flux	$6.5 \times 10^{14} \text{ photons / cm}^2\text{s}$
n-type doping density	$8 \times 10^{16} \text{ cm}^{-3}$

The carrier lifetime decreases due to increase in recombination through deep level traps generated because of irradiation. The performance of photodetector depends on the lifetime of photoexcited carriers. The effective carrier lifetime (τ_{eff}) is given by [12],

$$\frac{1}{\tau_{eff}} = \frac{1}{\tau_{SRH}} + \frac{1}{\tau_R} + \frac{1}{\tau_{Aug}} + \frac{2S}{d} \quad (2)$$

where τ_{SRH} is the Shockley-Read-Hall lifetime, τ_{Aug} is Auger lifetime, τ_R is the radiative recombination lifetime and 'S' is the surface recombination velocity. The increased trap density results in increase in trap assisted non-radiative recombination and reduces the overall lifetime of the carriers. The Shockley-Read-Hall lifetime is given by [2],

$$\tau_{SRH} = \frac{1}{\sigma_n v_{th} N_{trap}} \quad (3)$$

where σ_n is the capture cross section, N_{trap} is the trap density and the thermal velocity of charge carrier (U_{th}) in n-type $Hg_{1-x}Cd_xTe$ alloy is given by [2],

$$U_{th} = \sqrt{\frac{8KT}{\pi m_n^*}} \tag{4}$$

The carrier lifetime has an effect on photoconductive current gain of the HgCdTe detector. The photoconductive current gain is defined as the ratio of the carrier lifetime, τ_{eff} , to the transit time of carriers, τ_{tr} . The expression for photoconductive current gain (g) can be written as [2],

$$g = \frac{\tau_{eff}}{\tau_{tr}} \tag{5}$$

The gain of the photoconductor is shown to be affected by non-radiative recombination through trap centers. The photoconductive gain is plotted as a function of trap density in Fig. 8. The responsivity and detectivity which depends on the gain of the PC detector also decreases. The responsivity variation with increasing trap density is shown in Fig. 9. The responsivity decreases with increasing trap density. The responsivity, R_V of an HgCdTe photoconductor is given by [12],

$$R_V = \frac{\eta_e \lambda q g r_d}{hc} \tag{6}$$

where η_e is the quantum efficiency, 'g' is the photoconductive current gain. The detectivity (D^*) which characterizes the signal-to-noise ratio of the detector also decreases with the increase in trap density and it is expressed as [2],

$$D^* = \frac{R_V \sqrt{I_w B}}{V_n} \tag{7}$$

where B is the bandwidth of the detector and V_n is the noise voltage.

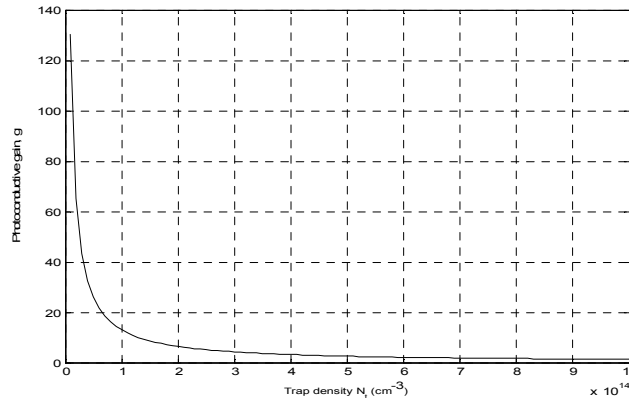


Fig. 8. Variation of Photoconductor Gain with SRH Trap Density for an Applied Voltage of 1.17 V in the Absence of Surface Recombination.

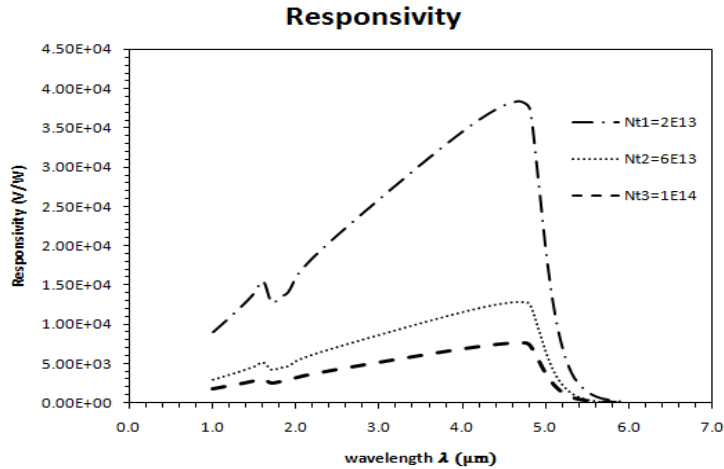


Fig. 9. Variation of Responsivity with Operating Wavelength for Different Trap Densities.

4. Analytical Model

The radiation induced deep trap centers are considered to be better recombination centers. The concentration of radiation induced deep trap centers is a function of material, energy of radiation, and the amount of radiation exposure. The kinetics of generation of deep trap centers due to radiation is considered to be a first order rate equation, as given below,

$$N_A(t) = N_{oe} + N_{se} (1 - \text{Exp}(t/t_M)) \quad (8)$$

where N_{oe} is the concentration of initial deep trap centers. N_{se} is the saturation value of the radiation induced deep trap centers and t_M is the time constant. N_{se} and t_M are constants which depend on the intensity of radiation. Figure 10 shows the variation of trap density with time for different radiation measurements. The markers indicate the variation of trap density with time as estimated from simulations and the solid line represents the fitting curve plotted using the analytical model developed. By using least squares fitting method in MATLAB, the values of N_{se} , t_M for different temperatures are extracted as shown in Table 3. The initial value of trap density during irradiation N_{oe} , for all temperature measurements is found to be $1 \times 10^{13} \text{ cm}^{-3}$.

Table 3. The Saturation Value of Radiation Induced Deep-Trap Centers and the Time Constant for Different Temperature Measurements.

Temperature (°C)	Time constant, t_M (hrs)	Saturation value of trap density, $N_{se} (\text{cm}^{-3})$
45	5.40	5.0×10^{13}
55	4.42	5.4×10^{13}
70	3.04	6.2×10^{13}
90	2.03	6.8×10^{13}

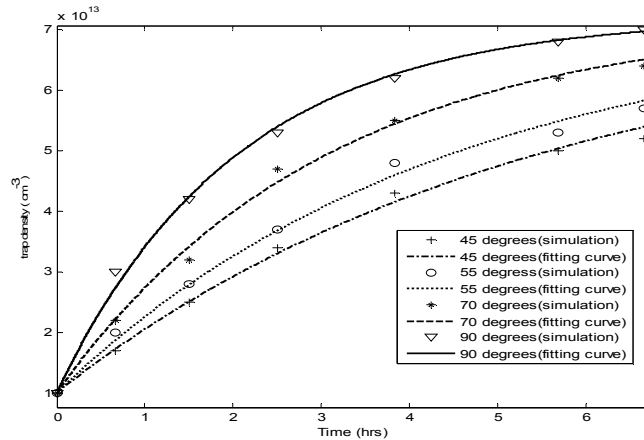


Fig. 10. Variation of Trap Density with Time.

5. Conclusions

In this work, the characteristics of temporal drift in the spectral responsivity of HgCdTe photodetectors have been investigated and found to have an origin different from what has been reported in literature. The Dewar in which the detector is housed had been completely evacuated before the drifts are observed. This ensures that drifts observed have nothing to do with ice-formation. The source of drift as proposed in this paper is more critical owing to the difficulties in acquisition of infrared temperature measurements, however not the ice-formation. In this paper, it is demonstrated that the source of new drift is due to charge trapping effects and generation of radiation induced deep trap centers, which are meta-stable in nature. Experiments and simulations have been carried out to ascertain the cause of the drift and a theoretical model has been proposed which explains the characteristics of the drift phenomenon. It has been shown that due to the variation of radiation induced deep trap centers, effective carrier lifetime in the semiconductor changes and hence the drift effects are being observed.

Acknowledgment

Authors thank Dr. Sanjay Gupta, CTO, IIT Kanpur, for providing the necessary equipment's in conducting the experiments.

References

1. Rogalski, A. (2005). HgCdTe infrared detector material: History, status, and outlook. *Reports on Progress in Physics*, 68(10), 2267-2336.
2. Dwivedi, A.D.D.; and P. Chakrabarti (2007). Modeling and Analysis of the Photo-conductive detectors based on $Hg_{1-x}Cd_xTe$ for free space optical Communication. *Optical and Quantum Electronics*, 39(8), 627-641.

3. Zhang, J.; Westerhout, R.J.; Tsen, G.K.O.; Antoszewski, J.; Yang, Y.; Dell, J.M.; and Faraone, L. (2008). Sidewall Effects of MBE Grown CdTe for MWIR HgCdTe Photoconductors. *Conference on Optoelectronic and Microelectronic Materials and Devices (COMMAD '08), Sydney, Australia*.
4. Siliquolini, J.F.; Musca, C.A.; Nener, B.D.; and Faraone, L. (1995), Temperature dependence of Hg_{0.68}Cd_{0.32}Te infrared photoconductor performance. *IEEE Transactions on Electron Devices*, 42(8), 1441-1448.
5. Theocharous, E.; and Theocharous, O.J. (2006), Practical limit of the accuracy of radiometric measurements using HgCdTe detectors. *Applied Optics*, 45(30), 7753-7759.
6. Theocharous, E. (2006). On the stability of the spectral responsivity of cryogenically cooled HgCdTe infrared detectors. *Infrared Physics and Technology*, 48(3), 175-180.
7. Hatch, S.D.; Musca, C.A.; Becker, C.R.; Dell, J.M.; and Faraone, L. (2011). Photoresponse in photoconductor devices fabricated from HgTe-HgCdTe superlattices. *Applied Physics Letters*, 98(4), 043505-1- 043505-3.
8. Rogalski, A.; Antoszewski, J.; and Faraone, L. (2009). Third-generation infrared photodetector arrays. *Journal of Applied Physics*, 105(9), 091101-1- 091101-44.
9. Kodolbas, A.O.; Eray, A.; and Oktu, O. (2001). Effect of light-induced metastable defects on photo-carrier lifetime. *Solar Energy Materials and Solar Cells*, 69(4), 325-337.
10. Norton, P. (2002). HgCdTe infrared detectors. *Opto-Electronics Review*, 10(3), 159-174.
11. Pierre-Yves, E. (2009). *HgCdTe Auger -Suppressed Infrared Detectors under Non-Equilibrium Operation*. Ph.D. Thesis, University of Michigan.
12. Pal, R.; Bhan, R.K.; Chhabra, K.C.; and Agnihotri, O.P. (1996). Analysis of the effect of surface passivant charges on HgCdTe photoconductive detectors. *Semiconductor Science and Technology*, 11(2), 231-237.